Characterisation of the multi-scale fabric features of high plasticity clays

Géotechnique Letters

Characterisation of the multi-scale fabric features of high plasticity clays

--Manuscript Draft--

Manuscript Number:	
Full Title:	Characterisation of the multi-scale fabric features of high plasticity clays
Article Type:	Themed Issue: Micro to Macro Mechanics
Corresponding Author:	Simona Guglielmi ITALY
Corresponding Author Secondary Information:	
Corresponding Author's Institution:	
Corresponding Author's Secondary Institution:	
First Author:	Federica Cotecchia
First Author Secondary Information:	
Order of Authors:	Federica Cotecchia
	Simona Guglielmi
	Francesco Cafaro
	Antonio Gens
Order of Authors Secondary Information:	
Abstract:	The letter describes an investigation of the microstructural features of a high-plasticity clay, in both its natural conditions and reconstituted in the laboratory. Scanning electron microscopy is used to characterise the fabric; image processing of the micrographs delivers a quantitative assessment of the orientation of particles. Despite their identical composition, the natural and the reconstituted clay have experienced different deposition and loading history, generating different microstructural features that are shown to underlie their differences in state. For both clays, the fabric is shown to be well oriented at medium magnification. However, SEM observations at larger magnification, and the corresponding image processing results, reveal that areas of random particle aggregation alternate with zones with layers of perfectly oriented particles, providing evidence of multi-scale fabric features, which make fabric characterisation dependent on the scale of analysis. This peculiar fabric character is also identified in the two clays after 1D compression to high pressures, showing that, due to loading, fabric undergoes a complex re-organization but the index of fabric orientation remains largely constant. Thereby, it is concluded that electrostatic and short-range forces, rather than mechanical, are strongly influential during compression thus explaining the isotropic hardening observed in laboratory tests.

Dear Editor,
please receive the original paper entitled:

"Characterisation of the multi-scale fabric features of high plasticity clays"

Federica Cotecchia, Simona Guglielmi*, Francesco Cafaro*, Antonio Gens°*

** Department of Civil, Environmental, Land, Building Engineering and Chemistry, Politecnico di Bari, Bari, ITALY*
° Departamento de Ingeniería del Terreno, Universitat Politécnica de Catalunya, Barcelona, SPAIN

for consideration for the themed issue of Géotechnique Letters "Latest Findings on Micro to Macro Mechanics of Geomaterials".

The letter deals with the investigation of the microstructural features of high plasticity clays. Scanning electron microscopy and image processing are used for the qualitative and quantitative assessment of the clay fabric, while X-ray micro-analysis and swelling tests are adopted for estimating the bonding strength.
The microstructural analyses are carried out on both the natural clay and on the clay reconstituted in the laboratory, allowing to identify the microstructural differences underlying the differences in state. Moreover, the evolution of clay microstructure upon 1D compression of both the clays is investigated. Peculiar features of the clay fabric are outlined, providing evidence of its multi-scale architecture.

Looking forward to receiving from you a positive reply, we send our kindest regards.
Federica Cotecchia, Simona Guglielmi, Francesco Cafaro, Antonio Gens

Characterisation of the multi-scale fabric features of high plasticity clays

Federica Cotecchia

Department of Civil, Environmental, Land, Building Engineering and Chemistry, Politecnico di Bari, Bari, Italy

Orcid:0000-0001-9846-4193

Simona Guglielmi (*)

Department of Civil, Environmental, Land, Building Engineering and Chemistry, Politecnico di Bari, Bari, Italy

Orcid:0000-0003-0416-6836

Francesco Cafaro

Department of Civil, Environmental, Land, Building Engineering and Chemistry, Politecnico di Bari, Bari, Italy

Orcid:0000-0001-5076-8606

Antonio Gens

Departamento de Ingeniería del Terreno, Universitat Politécnica de Catalunya, Barcelona, Spain

Orcid:0000-0001-7588-7054

(*) Full contact details of corresponding author.

Department of Civil, Environmental, Land, Building Engineering and Chemistry, Politecnico di Bari, Bari, Italy – Via Edoardo Orabona, 4, 70126 Bari (BA), Italy

+39 080 5963363

simona.guglielmi@poliba.it

Abstract

The letter describes an investigation of the microstructural features of a high-plasticity clay, in both its natural conditions and reconstituted in the laboratory. Scanning electron microscopy is used to characterise the fabric; image processing of the micrographs delivers a quantitative assessment of the orientation of particles.

Despite their identical composition, the natural and the reconstituted clay have experienced different deposition and loading history, generating different microstructural features that are shown to underlie their differences in state. For both clays, the fabric is shown to be well oriented at medium magnification. However, SEM observations at larger magnification, and the corresponding image processing results, reveal that areas of random particle aggregation alternate with zones with layers of perfectly oriented particles, providing evidence of multi-scale fabric features, which make fabric characterisation dependent on the scale of analysis.

This peculiar fabric character is also identified in the two clays after 1D compression to high pressures, showing that, due to loading, fabric undergoes a complex re-organization but the index of fabric orientation remains largely constant. Thereby, it is concluded that electrostatic and short-range forces, rather than mechanical, are strongly influential during compression thus explaining the isotropic hardening observed in laboratory tests.

Keywords chosen from ICE Publishing list

clays; fabric/structure of soils; microscopy

List of notation

A	clay activity
CF	clay fraction
CRS	constant rate of strain oedometer test
C_s	swelling index
C_s*/C_s	swell sensitivity
e	void ratio
L	index of fabric orientation
OCR	overconsolidation ratio: σ'_p/σ'_v
OED	conventional oedometer test
PI	plasticity index
S_σ	Stress Sensitivity
w	water content
YSR	yield stress ratio: σ'_y/σ'_v
$\sigma*_e$	equivalent vertical effective stress on the ICL
σ'_p	vertical (geological) preconsolidation pressure
σ'_v	vertical effective stress

σ'_y vertical effective stress at yield

1. Introduction

This letter discusses the features of the microstructure of a high plasticity clay in its natural overconsolidated state, after one-dimensional (1D) compression in the laboratory (lab), and when reconstituted and also subjected to 1D compression (Burland, 1990). In this way, the microstructure corresponding to the different macro-states (void ratio, e, versus vertical effective stress, σ'_v) achieved by the clay through either a geological or a lab history (Leroueil & Vaughan, 1990; Cotecchia & Chandler, 2000) is investigated. The micro-scale investigation has made use of scanning electron microscopy (SEM), image processing of the micrographs at different magnifications, X-ray micro-analysis (Energy Dispersive X-ray Spectroscopy, EDS in the SEM) and, for the bonding strength, swelling tests.

The presented work is part of a research aimed at connecting the features of clay macro-behaviour (macro-mechanics) to the clay microstructure and history (e.g. Delage and Lefebvre, 1984; Hattab et al., 2013; Lima et al, 2008). Also, the research results are intended to support the modelling of clays in the framework of micro-mechanics, that must account for complex coupled chemo-physical processes at colloidal scale (e.g. Ebrahimi et al., 2012 and 2014, Anandarajah, 2000; Yao and Anandarajah, 2003, Ebrahimi et al., 2016; Liu et al., 2015; Sjoblom, 2016).

2. Composition, history and macro-behaviour of the clay

The investigated natural clay is the stiff Pappadai clay, deposited in the early Pleistocene in a quiet marine environment, with reducing conditions at the sea floor. The mineralogical composition and the index properties of the clay are reported in Table 1. It is mainly illitic, but includes a significant amount of smectite, interstratified illite-smectite and carbonatic silt.

For the geological history of the natural clay and the macro-behaviour of both the natural and the reconstituted clay, reference is made to Cotecchia & Chandler (1995 and 1997). A few aspects of the clay macro-behaviour, which characterize the macro-effects of some clay micro-features, are briefly recalled hereafter.

The state of the natural clay, A in the compression plane in Figure 1, results from overconsolidation due to unloading (OCR= σ'_p/σ'_{v0} = 3). When subjected to oedometric compression in the lab (Figure 1), the clay exhibits gross yield at σ'_y about twice σ'_p (yield stress ratio, YSR=$\sigma'_y/\sigma'_{v0} \cong 2\cdot$OCR) as result of diagenesis under burial, which has increased the strength of the clay microstructure.

Upon reconstitution and one-dimensional compression, the clay follows a compression curve to the left of the gross yield state of the natural clay (Figure 1), whose microstructure, achieved through the geological history, allows for e-σ'_v states in the 'structure permitted space' (Leroueil & Vaughan, 1990).

The swell sensitivity, i.e. C_s*/ C_{si} (Schmertmann, 1969), is about 2.5 and is indicative of a higher strength of the natural clay bonding with respect to that of the reconstituted, most likely due to diagenesis. For the undisturbed natural clay, the stress sensitivity S_σ, σ'_y/σ^*_e ($\cong p'_{yis}/p^*_{yis}$ in isotropic compression, Cotecchia and Chandler, 2000) equals 3.5 (Figure 1).

Upon compression, the swell sensitivity of the natural clay drops to 1 soon after gross yield ($C_s^*/C_{s,py}$, Figure 1), but S_σ decreases only gradually. Accordingly, the state of the natural clay keeps lying to the right of the ICL up to high pressures. The clay microstructure is an internal variable of the hardening function in several constitutive laws (e.g. Rouainia & Wood, 2000; Baudet & Stallebrass 2004). Cotecchia & Chandler (2000) proposed that S_σ, function of the plastic volumetric strain, $\varepsilon_v{}^p$, may be suited to represent the microstructure effects on the clay gross yield hardening. They support this proposal by means of experimental data for several clays, including Pappadai clay, showing that the gross yield surface of the tested materials can be normalized by the function $S_\sigma(\varepsilon_v{}^p)\cdot p_e^*(e)$ (where p_e* is the equivalent pressure for the current void ratio of the reconstituted clay). Therefore, an isotropic volumetric hardening function, equal to the product of the current stress sensitivity of the clay times the hardening function of the reconstituted clay (e.g. the Cam Clay hardening function; Schofield & Wroth 1968), appears to match the gross yield hardening of Pappadai clay (Figure 2).

3. Microstructure of the natural and reconstituted clay

The analysis of the clay microstructure concerned vertical fractures of freeze-dried specimens, by means of SEM (gold coated) and Field Emission SEM (FESEM, carbon coated), as discussed by Cotecchia & Chandler (1998), Cotecchia et al. (2016) and Guglielmi et al. (2018). The technique used for the digital image processing of the micrographs is operator-independent. It is fully discussed by Martinez-Nistal et al. (1999) and Mitaritonna et al. (2014), and it is based on the thinning of the elongated bright regions across the micrograph, which represent the edges of either particles, or particle aggregates (e.g. Figure 3). The thinning results in a field of vectors of varying orientation, processed to derive both a histogram of the detected particle orientations and a scalar “index of fabric orientation”, L (e.g. Figure 3). L ranges between 0.21 and 1 for “medium to very oriented fabric”, and is lower than 0.15 for “randomly oriented fabric”.

The reconstituted clay reaches state A* in Figure 1 (e=1.28; σ'_v=20kPa) through compression from slurry in the consolidometer, up to σ'_p=200kPa, and swelling. When investigated at 10^3 medium magnification (e.g. Figure 4), its fabric is found to match a repetitive pattern. This is formed of stacks, where densely packed domains are in either face to face, or edge to edge contact, which alternate with either macro-pores, or arrangements of non-oriented particles/domains (mostly in edge to face contact). The repetitiveness of these fabric features suggests that the medium magnification provides a representative view of the fabric on the whole. This fabric has been considered quite oriented by Cotecchia and Chandler (1997 and 1998) on a qualitative basis. Image processing, carried out recently for several medium magnification micrographs, confirms this identification, providing direction histograms like that in Figure 4, with L in the range 0.23-0.27.

The medium magnification fabric of the overconsolidated natural clay, whose state is A (e=0.88; σ'_v=414kPa) in Figure 1, appears repeatedly as a dense packing of massive aggregates (Figure 3). These are either domains arranged in stacks, or forming bookhouse arrangements, the latter through edge to edge and edge to face contacts. Also chaotic particle aggregates, macropores and unbroken micro-fossils can be found buried in the fabric. Cotecchia and Chandler (1997 and 1998) considered this fabric well oriented on qualitative basis. The image processing (e.g. overlay in Figure 3a) confirms, again, this qualitative finding, providing direction histograms of the type in Figure 3, with L in the range 0.24-0.37. Therefore, irrespective of the different deposition environment, history and current state, both the natural and the reconstituted clay are shown to possess massive well oriented fabrics, once the analysis of the particle orientation concerns vertical fractures of size equal to, or larger than 10^4 μm^2. It is deduced that, at the micro-scale, the clay representative element volume, REV, to be investigated in order to assess the overall fabric features, is the cubic volume subtended by a surface of size10^4 μm^2, which corresponds to 10^{-3} mm^3.

A high degree of fabric orientation is achieved by the reconstituted clay already by σ'_v=200kPa. The main differences between the fabrics at A and A* concern: i) the bonding, that is diagenized in the natural clay, as indicated by the detection, through X-ray micro-analysis, of an amorphous calcite film binding the particles (Cotecchia & Chandler 1997); ii) the size and quantity of the macro-pores (μm) and the density of the domain aggregates; iii) the complexity of the clay fabric, which appears higher for the natural clay, including more frequent chaotic aggregations.

When comparing the medium magnification micrographs for the reconstituted clay at A* with those for the reconstituted clay compressed to σ'_v=22MPa (state C*, Figure 1), the difference in overall fabric density is evident, given the absence of macro-pores and the thicker size of the massive layers of oriented particles in C* (Figure 5). Conversely, a variation in fabric orientation cannot be detected. Image processing confirms that the average fabric orientation of the reconstituted clay does not increase with the one-dimensional compression, since L keeps values about 0.24. A similar finding was reported by Mitaritonna et al. (2014) for reconstituted Lucera clay, when one-dimensionally compressed from σ'_v=140kPa to 1900kPa. The authors also show that the observed similarity in fabric orientation corresponds to a constancy in elastic stiffness anisotropy. In particular, different elastic stiffness anisotropies are shown to correspond to the different steady degrees of orientation that the clay achieves in different constant η=q/p' compressions. Therefore, the authors suggest that the clay macro-behaviour at very small strains relates to the degree of orientation of the clay fabric detected at medium magnification, here recognized as the REV fabric.

The role of the REV fabric as internal variable of the clay small strain macro-behaviour can be extended to the large strain behaviour as shown in the following, based upon the reconstituted Pappadai clay data. As indicated above, the main change in REV fabric for the reconstituted Pappadai clay under one-dimensional compression (constant η=0.6) is the reduction in porosity, since the fabric orientation remains constant. This fabric evolution is therefore the internal process providing the reconstituted clay with a hardening function that is isotropic and volumetric, as suggested by the data in Figure 6, which show that the state boundary surface (SBS) of reconstituted Pappadai clay can be normalized by $p_e^*(=e^{(N^*-\nu)/\lambda^*})$.

For the natural clay, compression to state B (Figure 1), soon after gross yield, is observed to cause a major weakening of the natural bonding, given the recorded drop in C_s^*/ C_s. Figure 7 shows one of several medium magnification micrographs for the clay at this state, which suggest that gross yielding results in some fabric rearrangement, including the chaotic filling of macro-pores with particle aggregates. However, the REV fabric does not attain a higher orientation degree, as confirmed by the image processing index L (Figure 7).

With post-gross yield compression up to 25 MPa (state C), the natural REV fabric (Figure 8) is repeatedly formed by thickened stacks of face to face particles (probably result of the coalescence of original stacks), of extremely low porosity, interbedding chaotic fabric portions. The fabric is not significantly more oriented than before compression, as confirmed by the direction histogram in Figure 8 and the orientation index, L=0.345. Therefore, compression post-gross yield of the natural clay determines: i) a major reduction of the macro-pores and a probable reduction of the micro-pores within the aggregates (to be checked through mercury intrusion porosimetry); ii) the thickening of stacks, which are also distorted and include areas of turbulent particles/domains; iii) a minor increase of the REV fabric orientation. This recorded constancy in fabric orientation suggests that, also for the natural clay, the gross yield hardening may be function solely of the volumetric straining, as for the reconstituted clay. This appears to be confirmed by the normalization of the SBS of the natural clay through the function $S_\sigma(\varepsilon_v^p)\cdot p_e^*(\nu)$ in Figure 2 (Cotecchia & Chandler 2000). For the natural clay, the hardening law must comply also with the evolving strength of the clay structure, through the function $S_\sigma(\varepsilon_v^p)$.

For all the investigated clay states, the inspection of micrographs at higher magnification than the medium one (i.e. 10^4-10^5) shows that the local fabric orientation varies from a complete preferred orientation (c.p.o.; Sides and Barden, 1970), to a poor orientation (bookhouse, cardhouse or honeycomb). For example, Figures 9a and b, for the initial states of the reconstituted and the natural clay respectively, and Figures 10a, 10b, 10c, for the reconstituted and the natural clay at different stages of compression, show examples of fabric portions (10^{-6} mm^3) where the degree of orientation, L, drops below 0.21. Conversely, in the several c.p.o. fabric portions, L is found to be very high. Therefore, the fabric orientation is not uniform and the local phenomena taking place under one-dimensional compression may be classified in two categories: a) the coalescence of domains bringing about the thickening and compaction of particle stacks (c.p.o.); b) the shift of domains and aggregates, to achieve a denser fabric packing, preserving the original features of edge to edge and face to edge fabric aggregates (e.g. Figs. 9 and 10). Hence, the external loading seems to generate mostly a mechanical displacement of particle aggregates, rather than the collapse of face to edge and edge to edge particle/domain arrangements that are controlled by electrostatic or short-range forces. This finding may be of interest in the micro-modelling of clay behaviour.

4. Conclusions

The research findings reported here have highlighted the multi-scale nature of the clay fabric. The multi-scale analysis shows that, since the local features of the clay fabric detectable at high magnification are not uniform, it is necessary to characterize the REV of the micro-structure in order to assess the micro-scale source of the clay macro-response. For the clay under study, the REV size is 10^{-3} mm^3, whose analysis requires image processing of micrographs at 10^3 magnification.

The findings reveal the complexity of the fabric of the investigated multi-mineral clay, reconstituted in the laboratory, subjected to high consolidation stresses and diagenesis in its geological history. Despite the differences in fabric and bonding of the natural and reconstituted clay, though, the REV fabric orientation is constant with constant η compression up to high pressures, and flocculated fabric portions do not necessarily undergo collapse due to external loading. Such microstructural changes constitute the background of a volumetric isotropic gross yield hardening of both clays.

The multi-scale analysis of the natural clay fabric at very high pressures suggests that during compression, after a major weakening of bonding at gross yield, the micro-scale phenomena optimize the particle arrangement, which evolves into an alternation of slabs (c.p.o) and bookhouse fabric portions. Such fabric evolution allows the natural clay to keep void ratios higher than those of the reconstituted clay, at any pressure.

Acknowledgements

The authors thank Dr. Vito Summa and Dr. Antonio Lettino of the Institute of Methodologies for Environmental Analysis (IMAA) of the National Research Council (CNR) at Tito Scalo (PZ, Italy) for the use of the FESEM. They are also grateful to Dr. Angel Martinez-Nistal for the image processing of the micrographs.

References

Anandarajah A (2000) Numerical simulation of one-dimensional behaviour of a kaolinite. Géotechnique **50(5)**: 509–519.

Baudet BA and Stallebrass SE (2004) A constitutive model for structured clays. Géotechnique **54**: 269-278.

Burland J.B. (1990) On the compressibility and shear strength of natural soils. Géotechnique **40 (3)**: 329-378.

Cotecchia F and Chandler RJ (1995) The geotechnical properties of the Pleistocene clays of the Pappadai valley. Quarterly Journal of Engineering Geology **28**: 5-22.

Cotecchia F and Chandler RJ (1997) The influence of structure on the pre-failure behaviour of a natural clay. Géotechnique **47 (3)**: 523-544.

Cotecchia F and Chandler RJ (1998) One-dimensional compression of a natural clay: structural changes and mechanical effects. In *Proceedings of the 2nd International Symposium on Hard Soils Soft Rocks*, 103-114.

Cotecchia F and Chandler RJ (2000) A general framework for the mechanical behaviour of clays. Géotechnique **50**: 431-447.

Cotecchia F, Cafaro F, Guglielmi S (2016) Microstructural changes in clays generated by compression explored by means of SEM and Image Processing. Procedia Engineering **158**: 57-62.

Delage P and Lefebvre G (1984) Study of the structure of a sensitive Champlain clay and of its evolution during consolidation. Canadian Geotechnical Journal **21 (1)**: 21-35.

Ebrahimi D, Pellenq RJ-M, Whittle AJ (2012) Nanoscale elastic properties of montmorillonite upon water adsorption. Langmuir **28 (49)**: 16855–16863.

Ebrahimi D, Whittle AJ, Pellenq RJ-M (2014) Mesoscale properties of clay aggregates from potential of mean force representation of interactions between nanoplatelets. The Journal of Chemical Physics **140 (15)**: 154309.

Ebrahimi D, Pellenq RJ-M, Whittle AJ (2016) Mesoscale simulation of clay aggregate formation and mechanical properties. Granular Matter **18 (3)**: 1–8.

Gens A and Nova R (1993) Conceptual bases for a constitutive model for bonded soils and weak rocks. In *Proceedings of the international conference on hard soils-soft rocks*, Athens, 483–494.

Guglielmi S (2018) Evolution of the clay micro-structure in compression and shearing loading paths. PhD Thesis, Polytechnic University of Bari.

Guglielmi S, Cotecchia F, Cafaro F, Gens A (2018) Microstructural changes underlying the macro-response of a stiff clay. Proceedings of the International Symposium on "Micro to MACRO Mathematical Modelling in Soil Mechanics" - Trends in mathematics (in print).

Hattab M, Hammad T, Fleureau J-M, Hicher P-Y (2013) Behaviour of a sensitive marine sediment: microstructural investigation. Géotechnique **63 (1)**: 71- 84.

Leroueil S and Vaughan PR (1990) The general and congruent effects of structure in natural soils and weak rocks. Géotechnique **40**: 467-488.

Lima A, Romero E, Pineda JA, Gens A (2008) Low-strain shear modulus dependence on water content of a natural stiff clay. In *Proceedings of XIV Congresso Brasileiro de Mecanica dos Solos e Engenharia Geotécnica*, 1763-1768.

Liu J, Lin CL, Miller JD (2015) Simulation of cluster formation from kaolinite suspensions. International Journal of Mineral Processing **145**: 38–47.

Martinez-Nistal A, Vinale F, Setti M, Cotecchia F (1999) A scanning electron microscopy image processing method for quantifying fabric orientation of clay geomaterials. Applied Clay Science **14**: 235-243.

Mitaritonna G, Amorosi A, Cotecchia F (2014) Experimental investigation of the evolution of elastic stiffness anisotropy in a clayey soil. Géotechnique **64 (6)**: 463-475.

Rouainia M and Muir Wood D (2000) A kinematic hardening constitutive model for natural clays with loss of structure. Géotechnique **50 (2)**: 315-321.

Schmertmann JH (1969) Swell sensitivity. Géotechnique **19**: 530-533.

Schofield AN and Wroth CP (1968) *Critical State Soil Mechanics*, Mc Graw-Hill Book Co., London.

Sides G and Barden L (1970) The microstructure of dispersed and flocculated samples of kaolinite, illite and montmorillonite. Canadian Geotechnical Journal **8**: 391-399.

Sjoblom KJ (2015) Coarse-Grained Molecular Dynamics Approach to Simulating Clay Behavior. Journal of Geotechnical and Geoenvironmental Engineering ASCE **142 (2)**: 1–6.

Yao M and Anandarajah A (2003) Three-Dimensional Discrete Element Method of Analysis of Clays. ASCE Journal of Engineering Mechanics **129 (6)**: 585–596.

Yu CY, Chow JK, Wang Y-H (2016) Pore-size changes and responses of kaolinite with different structures subject to consolidation and shearing. Engineering Geology **202**: 122–13.

List of Tables

List of Figures

Table 1. Index properties, mineralogy and initial state of natural Pappadai clay (after Cotecchia and Chandler, 1997).

Composition and physical properties	Specific gravity, G_s	2.75
	Clay fraction, CF	58%
	Liquid limit. LL	65%
	Plasticity index, PI	35%
	Activity, A	0.6
	Natural water content, w_0	≈31%
	In situ void ratio, e_0	0.88
	Carbonate content	28%
Mineralogy	Quartz	3%
	Feldspar	1%
	Carbonate	22%
	Dolomite	6%
	Kaolinite	12%
	Chlorite	14%
	Illite	20%
	Smectite	12%
	Interstratified	10%
	Total	100%

Figure 1

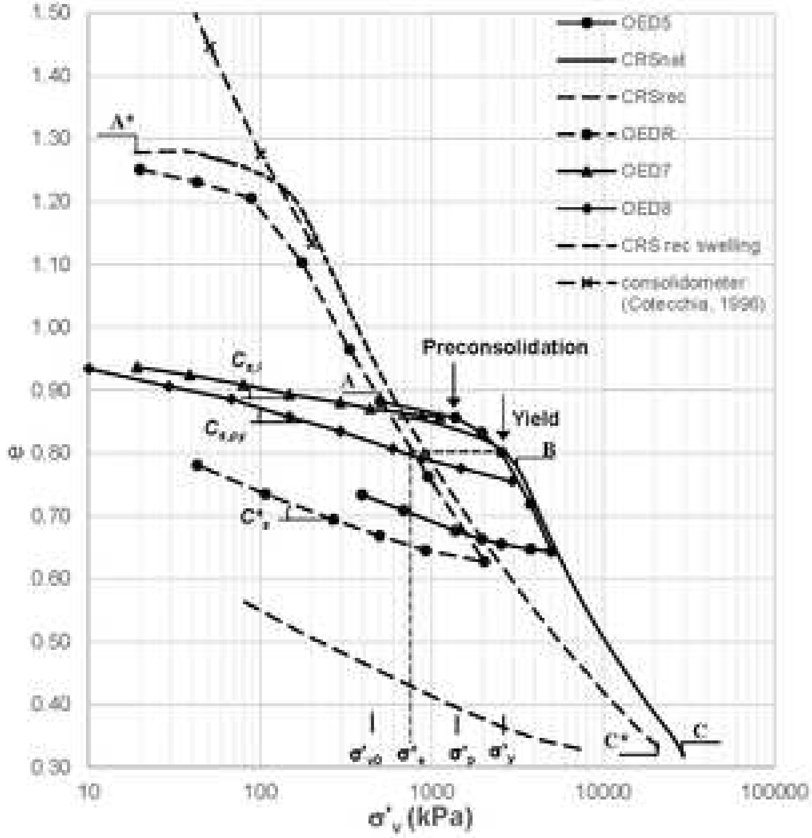
OED5
CRSnat
CRSrec
OEDR
OED7
OED8
CRS rec swelling
consolidometer (Cotecchia, 1996)
Preconsolidation
Yield
A*
A
B
C
C*
e
σ'v (kPa)
1.50
1.40
1.30
1.20
1.10
1.00
0.90
0.80
0.70
0.60
0.50
0.40
0.30
10
100
1000
10000
100000

Figure 2

Figure 2

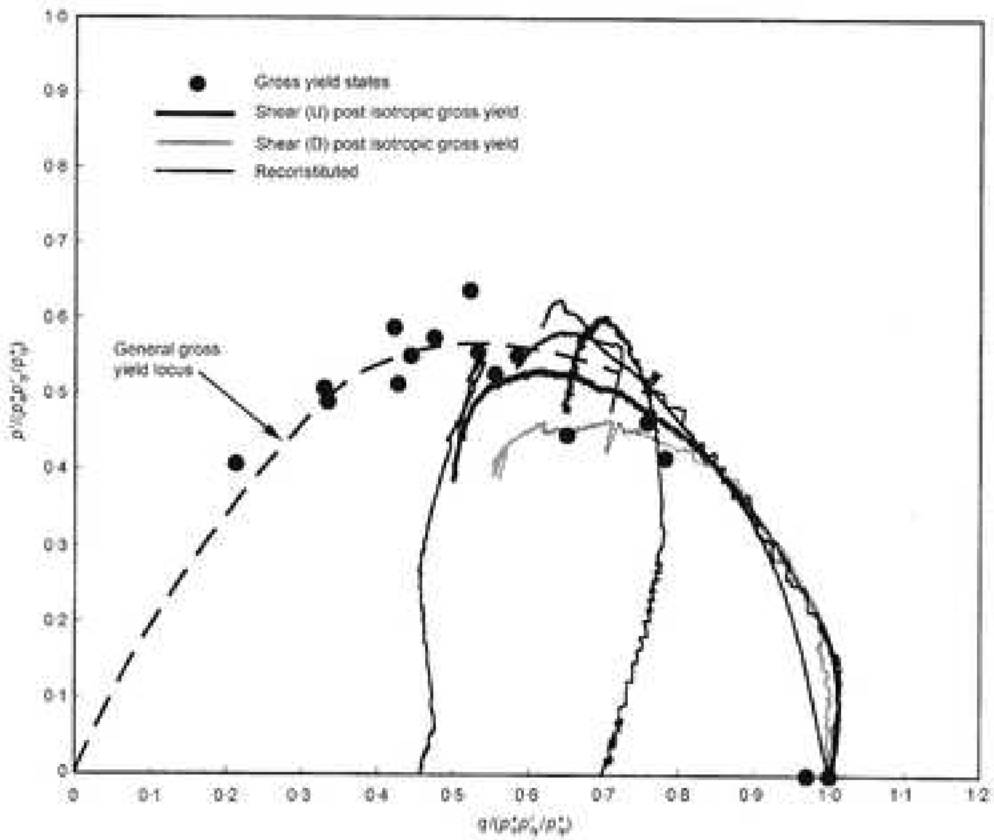

Figure 3

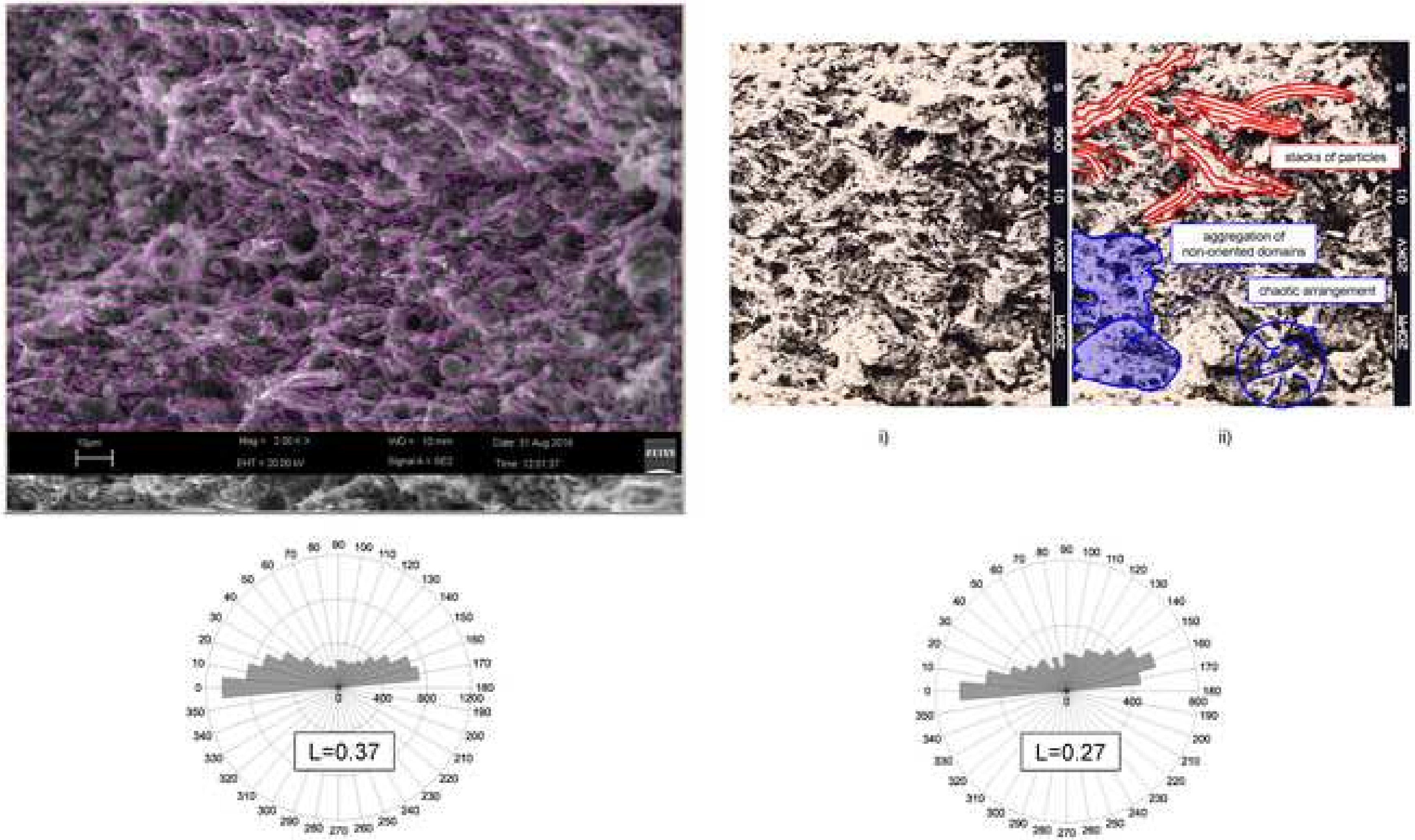
i)
ii)
stacks of particles
aggregation of
non-oriented domains
chaotic arrangement
L=0.37
L=0.27

a) b)

Figure 4

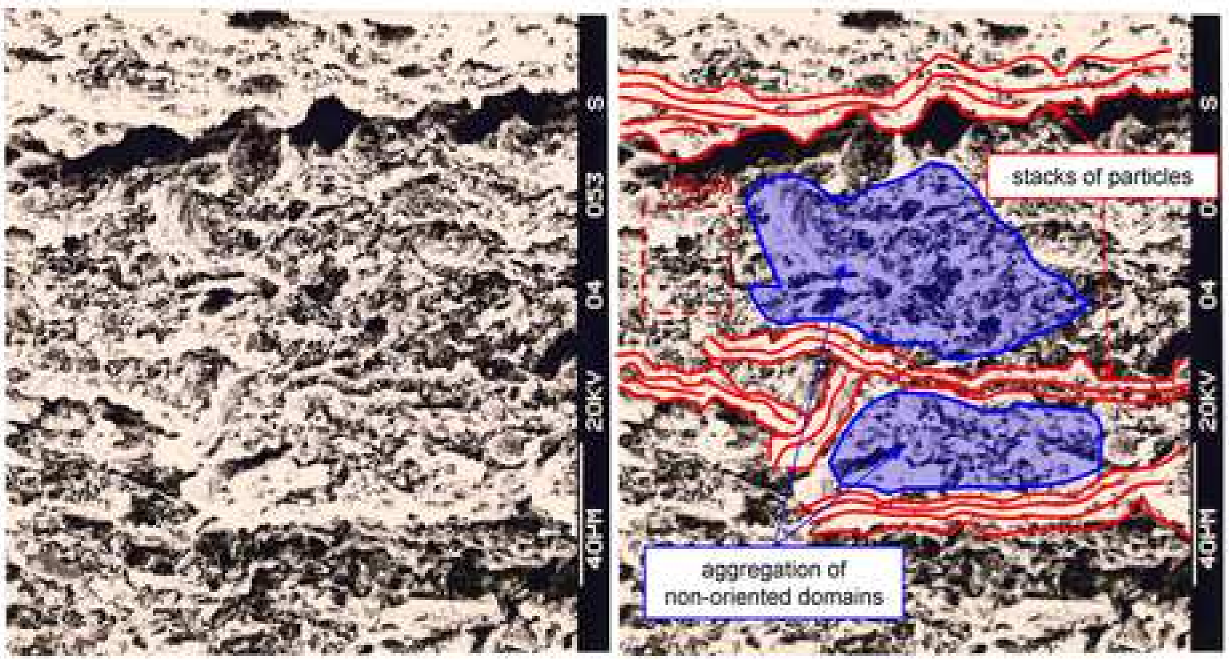
stacks of particles
aggregation of
non-oriented domains

i) ii)

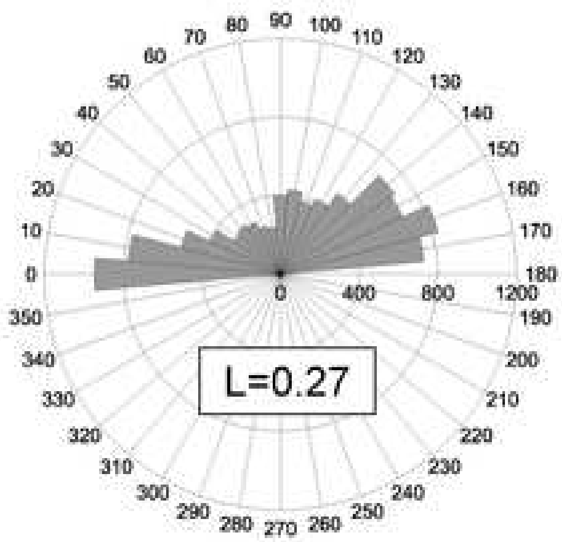
L=0.27
0
400
800
1200

Figure 5

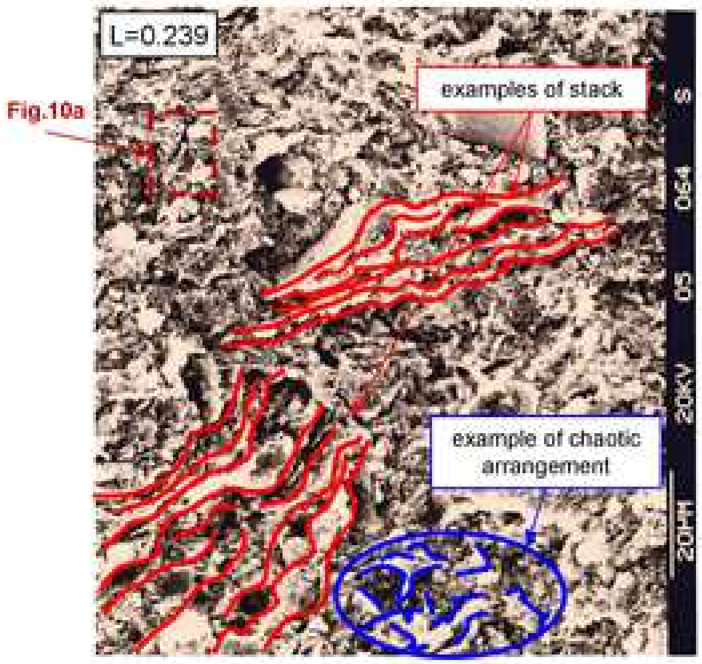
L=0.239
Fig.10a
examples of stack
example of chaotic arrangement
S 064 05 20KV 20μm

Figure 6

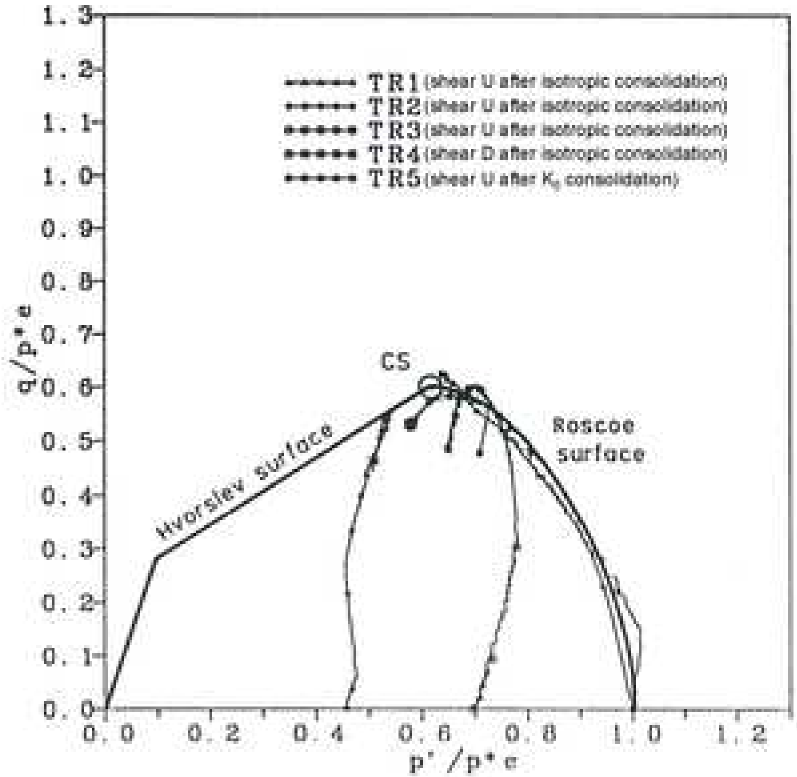
TR1 (shear U after isotropic consolidation)
TR2 (shear U after isotropic consolidation)
TR3 (shear U after isotropic consolidation)
TR4 (shear D after isotropic consolidation)
TR5 (shear U after K0 consolidation)
CS
Hvorslev surface
Roscoe surface
q/p*e
p'/p*e
0.0
0.1
0.2
0.3
0.4
0.5
0.6
0.7
0.8
0.9
1.0
1.1
1.2
1.3
0.0
0.2
0.4
0.6
0.8
1.0
1.2

Figure 7

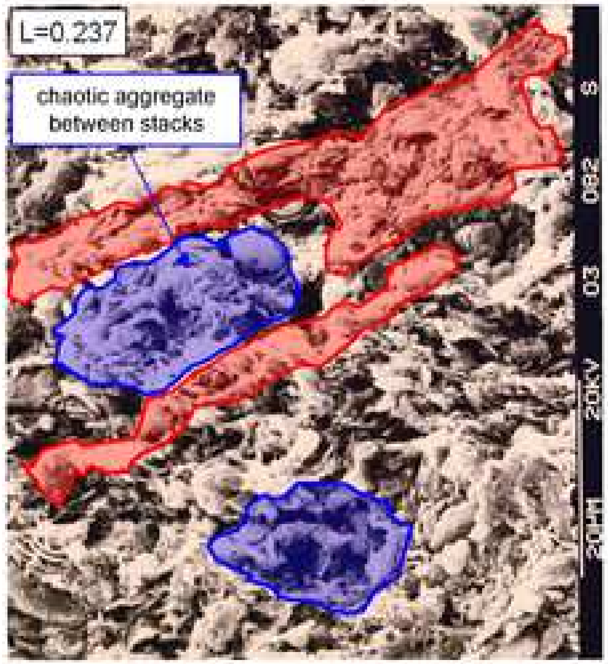

Figure 8

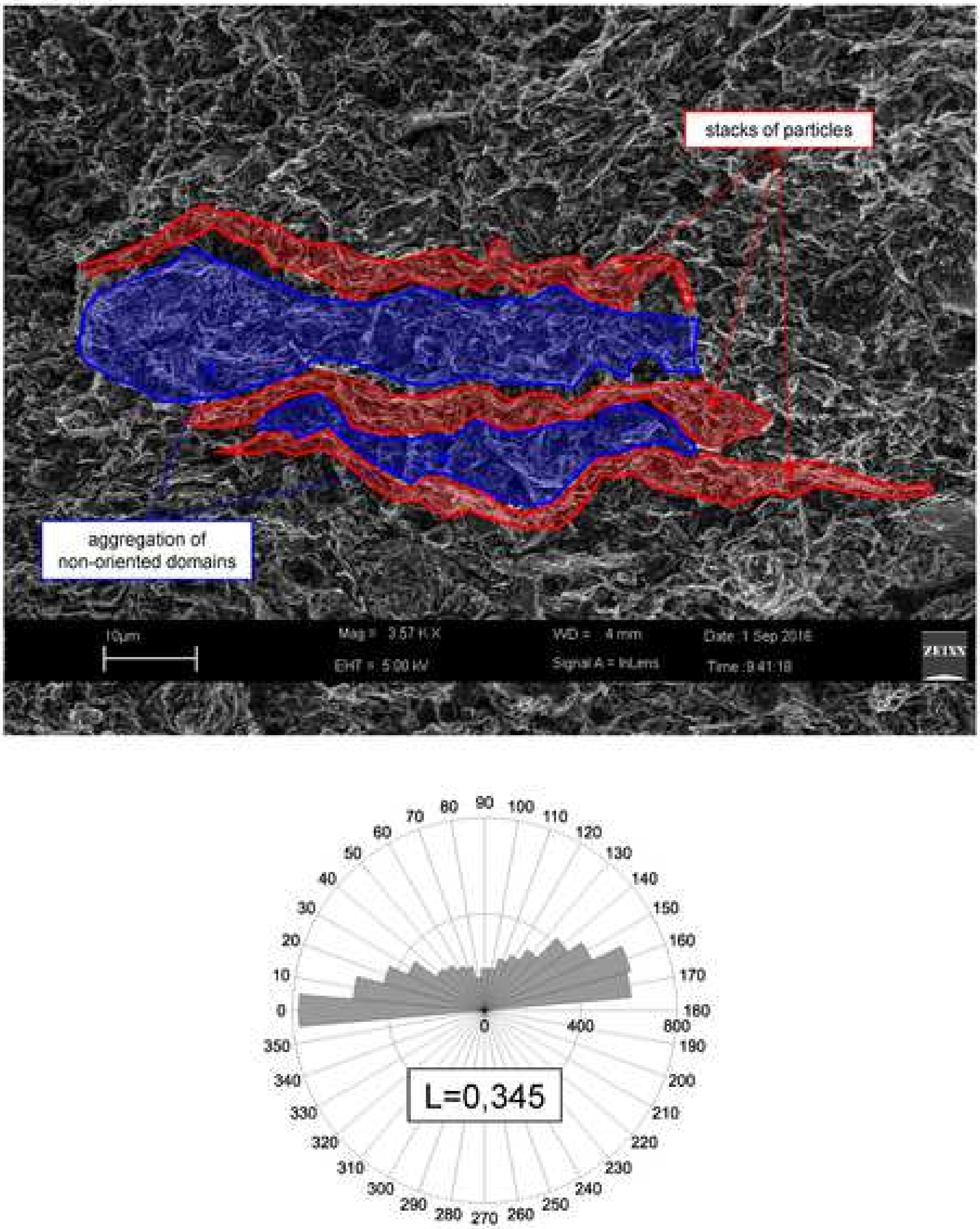
stacks of particles
aggregation of
non-oriented domains
10μm
Mag = 3.57 K X
EHT = 5.00 kV
WD = 4 mm
Signal A = InLens
Date :1 Sep 2016
Time :9:41:18
ZEISS
90
100
110
120
130
140
150
160
170
180
190
200
210
220
230
240
250
260
270
280
290
300
310
320
330
340
350
0
10
20
30
40
50
60
70
80
0
400
800
L=0,345

Figure 9

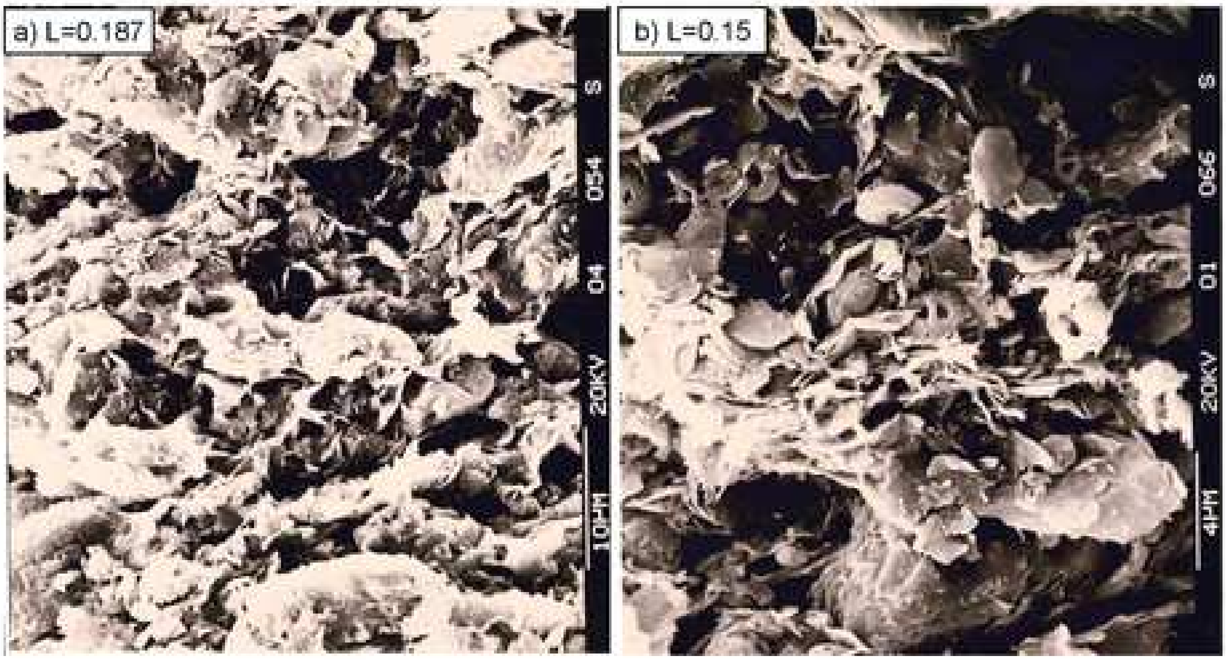

Figure 10 Click here to access/download;Figure;Figure 10.tiff

Figure 10